

Magnetic structure of erbium

H. Lin and M. F. Collins

Department of Physics, McMaster University, Hamilton, Ontario, Canada L8S 4M1

T. M. Holden and W. Wei

Neutron and Solid-State Physics, AECL Research, Chalk River, Ontario, Canada K0J 1J0

(Received 20 November 1991)

Elastic neutron scattering has been used to study the magnetic structure of erbium in an applied magnetic field of up to 2.8 T along the c axis. There are three major types of ordered structure: the cone phase, an intermediate-temperature phase with moments modulated both along the c axis and perpendicular to the c axis, and a phase at high temperatures where only the c component of the moment is ordered. Within these phases the modulation of the moments may lock in to the lattice. The field tends to stabilize the cone phase and to destabilize the intermediate phase. A lock-in structure with $\mathbf{q}=(1/4)\mathbf{c}^*$ appears in the cone phase for fields above 1.8 T. The presence of the field also greatly stabilizes the lock-in structure with $\mathbf{q}=(2/7)\mathbf{c}^*$ in both the intermediate- and the high-temperature phases.

I. INTRODUCTION

The magnetic ordering of erbium has been studied by use of neutron and x-ray magnetic scattering over the decades since the neutron-scattering experiments of Cable *et al.*¹ in the early 1960s. In the absence of an applied field, three distinct ordered states were found below the Néel temperature. In the high-temperature region (52–80 K), the moments are modulated sinusoidally along the c axis with wave vector $\mathbf{q}\approx 0.29\mathbf{c}^*$. As the temperature decreases, the modulation of the z component of the moments becomes increasingly squared-off and below 52 K the in-plane components of the moments order with the same periodicity as the z component of the moments. The wave vector \mathbf{q} decreases monotonically from about $0.29\mathbf{c}^*$ to $0.25\mathbf{c}^*$. Between 20 and 25 K, a commensurate structure with $\mathbf{q}=(1/4)\mathbf{c}^*$ is stable as a squared-up “alternating cone” phase. In the low-temperature region below 20 K, the z component of the moments aligns ferromagnetically and the xy components rotate uniformly with $\mathbf{q}=(5/21)\mathbf{c}^*$ to form a cone phase.

Later studies by Habenschuss *et al.*² showed the development of harmonics of the magnetic peaks in the higher temperature regions. A commensurate structure with $\mathbf{q}=(4/15)\mathbf{c}^*$ was observed at 33 K. The phase transition temperatures were not identical to those found by Cable *et al.*

The x-ray magnetic scattering study by Gibbs *et al.*³ in 1986 showed that there was a sequence of commensurate and incommensurate phase transitions in the intermediate-temperature region. The wave vectors of the commensurate structures lock in to certain rational-fractional values which can be described by $\mathbf{q}=n(4n-1)^{-1}\mathbf{c}^*$ with $n=2,3,4,5,6,\infty$. The temperature ranges of the lock-ins are up to 5 K wide. These structures were described by a c -axis spin-slip model,³ where the basic structure consists of four layers of spins parallel to z followed by four layers antiparallel to z . A

spin slip occurs when only three layers are aligned in the same direction. The spin slip occurs every n th block of layers and there is a net ferrimagnetic moment if n is even.

The structure in an applied magnetic field was studied by Rhyne and Pickart⁴ for a field along the a axis and by Atoji⁵ for a field of 2 T along the c axis. Recently an ultrasound investigation has been carried out in an applied field along the c axis.⁶

This paper presents neutron scattering studies of the structure of erbium in an applied magnetic field along the c axis. A brief account of parts of the work has already appeared.⁷ The results show that the effect of a field is to stabilize the cone phase at low temperatures and to produce a lock-in cone structure with $\mathbf{q}=(1/4)\mathbf{c}^*$. It also stabilizes the $\mathbf{q}=(2/7)\mathbf{c}^*$ phase in both the high-temperature phase [the c -axis-modulated (CAM) phase] and the intermediate-temperature phase. In contrast the field rapidly destroys the lock-in at $\mathbf{q}=(5/19)\mathbf{c}^*$. The experimental details and the formalism are described in Secs. II and III. Section IV gives experimental results with a description of the lock-in phase transitions, magnetic structures, and a magnetic phase diagram. Section V includes discussion and conclusions.

II. EXPERIMENTAL DETAILS

The single crystal, as originally supplied by Metal Research Ltd., was 2 mm thick, 6 mm wide, and 30 mm long. The lattice parameters of the hexagonal-close-packed structure were found to be $a=3.550$ Å and $c=5.600$ Å at 4.2 K. The sample was aligned with the (hhl) plane horizontal and mounted in a horizontal field magnet cryostat⁸ with a maximum field of 3 T. The field was orientated along the c axis of the crystal with an accuracy of $\pm 3^\circ$. The calibrated carbon temperature sensors were located on the aluminum sample holder, and the temperature was controlled to about 0.1 K.

The neutron diffraction measurements were carried out

on the N5 triple-axis spectrometer, in elastic scattering mode, at the NRU reactor of the Chalk River Laboratories. Silicon (111) reflections were used for both monochromator and analyzer. The horizontal collimation from the reactor to the detector was 33'-19'-24'-56'. The incident neutron wavelength was 2.37 Å and a pyrolytic graphite filter was placed in the scattered beam in order to reduce higher-order contamination. The resolution was typically 0.02–0.03 reciprocal lattice unit (r.l.u.).

Scans were taken by varying l along the $[11l]$ and $[00l]$ directions in reciprocal space. The $(1,1,l)$ peaks have a slightly larger width than the $(0,0,l)$ peaks. The $(1,1,0)$ peak has an asymmetric wing.

The measurements were normally performed with increasing temperature, because erbium shows hysteresis effects^{1,2} below 52 K. There were high torques on the sample from the magnetic field in some configurations; the horizontal alignment of the crystal was corrected as necessary.

The position and the integrated intensity of the Bragg reflections were determined by fitting the data to a Gaussian line shape. The value of q for a magnetic peak was taken relative to the position of the nearest nuclear Bragg peak. For determinations of the magnetic structure factor the magnetic intensity was normalized to the intensity of the nearest nuclear peak. A correction of the integrated intensity for a triple-axis spectrometer in the elastic mode was made following Cowley and Bates.⁹

The use of this relatively long wavelength to measure elastic scattering improves resolution for the position of a Bragg peak in reciprocal space, but increases extinction effects that systematically reduce the intensity of the strong peaks. Thus our measurements will underestimate the strength of the strong Bragg reflections, but will give good values for the strength of the weaker reflections.

III. FORMALISM

The measurements give the integrated intensities for nuclear peaks $I^n(\mathbf{Q})$ and for magnetic peaks $I^m(\mathbf{Q})$. The magnetic peaks have two components, one $I_z^m(\mathbf{Q})$ comes from the z component of the ordered moments and the other $I_{xy}^m(\mathbf{Q})$ comes from the xy component. By measuring the intensities of equivalent magnetic peaks in different directions it is possible to separate out these two components and to determine the magnitude of the magnetic structure factors:

$$F_z^m(\mathbf{Q}) = \sum_i m_{iz} \exp(i\mathbf{Q} \cdot \mathbf{R}_i)$$

and

$$\mathbf{F}_{xy}^m(\mathbf{Q}) = \sum_i \mathbf{m}_{ixy} \exp(i\mathbf{Q} \cdot \mathbf{R}_i),$$

where the sum is over the atoms i at position \mathbf{R}_i in the magnetic cell. m_{iz} and \mathbf{m}_{ixy} are the z component and the vector component in the xy plane, respectively, of the moment on the atom i . The intensity of the magnetic Bragg peaks is given by the sum of the two components:

$$I_z(\mathbf{Q}) = 0.0725c |f(\mathbf{Q})|^2 (1 - \hat{Q}_z^2) |F_z^m(\mathbf{Q})|^2 L(\mathbf{Q})$$

and

$$I_{xy}(\mathbf{Q}) = 0.0725c |f(\mathbf{Q})|^2 (1 + \hat{Q}_z^2) |\mathbf{F}_{xy}^m(\mathbf{Q})|^2 L(\mathbf{Q}),$$

where $f(\mathbf{Q})$ is the magnetic form factor, whose value we take from Stassis *et al.*,¹⁰ \hat{Q}_z is the direction cosine of \mathbf{Q} along z , and $L(\mathbf{Q})$ is the Lorentz factor. c is an instrumental constant which is determined by measurement of the nuclear intensities,

$$I^n(\mathbf{Q}) = c |F^n(\mathbf{Q})|^2 L(\mathbf{Q})$$

with

$$F^n(\mathbf{Q}) = \sum_i b_i \exp(i\mathbf{Q} \cdot \mathbf{R}_i)$$

when $b_i = 0.803 \times 10^{-12}$ cm is the nuclear scattering length of erbium.¹¹

IV. EXPERIMENTAL RESULTS AND DISCUSSIONS

A. Lock-in phase transitions

Figure 1 summarizes our data for the temperature dependence of the wave vector \mathbf{q} at different fields. For $T > 54$ K, the value of q was determined from the $(1,1,q)$ peak since the moments in the basal plane were no longer ordered. For $T < 54$ K, an average of the peak positions of $(0,0,2-q)$, $(1,1,q)$, and $(1,1,3q)$ was used, though in a field only the position of the $(0,0,2-q)$ peak was measured systematically. The error is within ± 0.002 r.l.u.

In zero field, q locks into the rational fractions $5/21$, $1/4$, and $5/19$ in the temperature range of 4.2–20, 21–27, and 30–34 K, respectively. We did not see other lock-ins found by the x-ray magnetic scattering.³ Comparison with several similar experiments from Refs. 1–4 shows a sample dependence of the lock-ins in this temperature region.

In Fig. 2(a) we show more detailed measured lock-ins from the $(0,0,2-q)$, $(1,1,q)$, and $(1,1,3q)$ reflections in zero field. The data show that the lock-ins occur in the same temperature range independent of the reciprocal-lattice vector \mathbf{Q} , and are therefore three dimensional. This has been suggested from recent magnetization and ac susceptibility experiments by two different groups.^{12,13} Since the $(0,0,2-q)$ reflection corresponds to xy components of the moments and $(1,1,q)$ maximizes the z component of the moments, the evidence of the three-dimensional lock-ins indicates that the spins in the basal plane and along the c axis are coupled. There seems to be a systematic difference between the values of q obtained from $(0,0,2-q)$ and $(1,1,q)$ although in both cases the position of the magnetic peaks were determined relative to the position of the nearest nuclear peak. The values of q from $(0,0,2-q)$ are about 0.5% larger. The most accurate determination of the wave vector by Gibbs *et al.*³ suggest that the lock-in at around 25 K, for instance, is exactly at one quarter, so it is likely that there is a small systematic error in our $(0,0,2-q)$ data.

When a field is applied along the c axis, the lock-ins at $1/4$ and $5/19$ are destroyed. Figure 2(b) shows the evolution of \mathbf{q} with field for temperatures corresponding to the center and the boundaries of the region of the

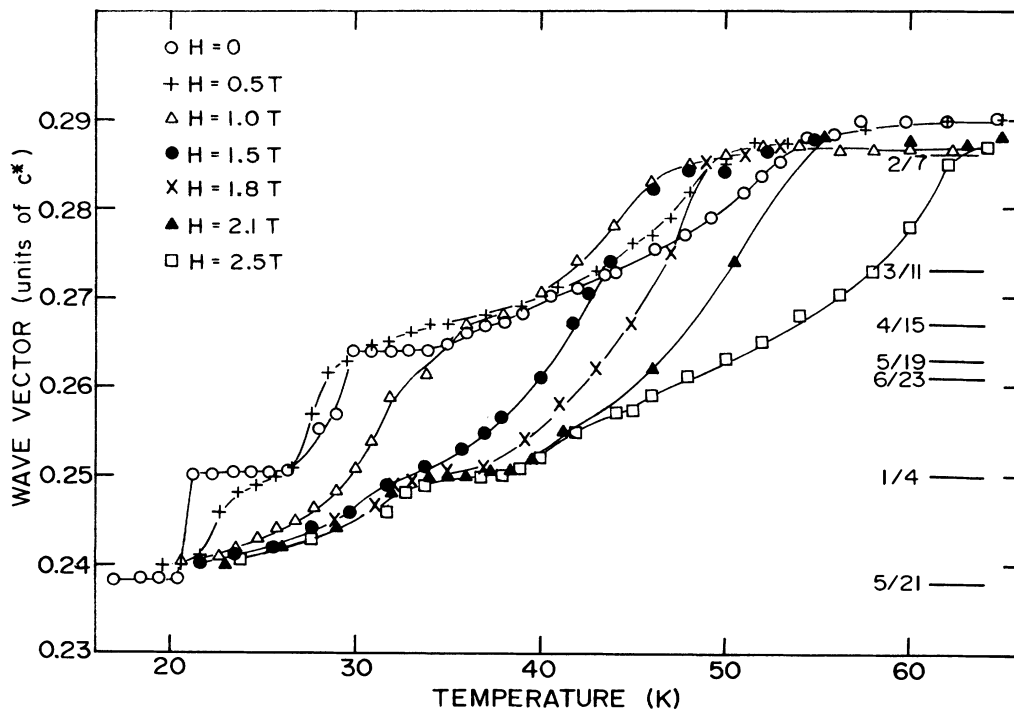


FIG. 1. The magnitude of the wave vector q as a function of temperature at different fields applied along the c axis. Lock-ins at $5/21$, $1/4$, and $5/19$ in zero field, at $1/4$ in a field of above 1.8 T and at $2/7$ in a field can be seen. The rational fractions on the right are the zero field lock-ins predicted by the c -axis spin-slip model (Ref. 3).

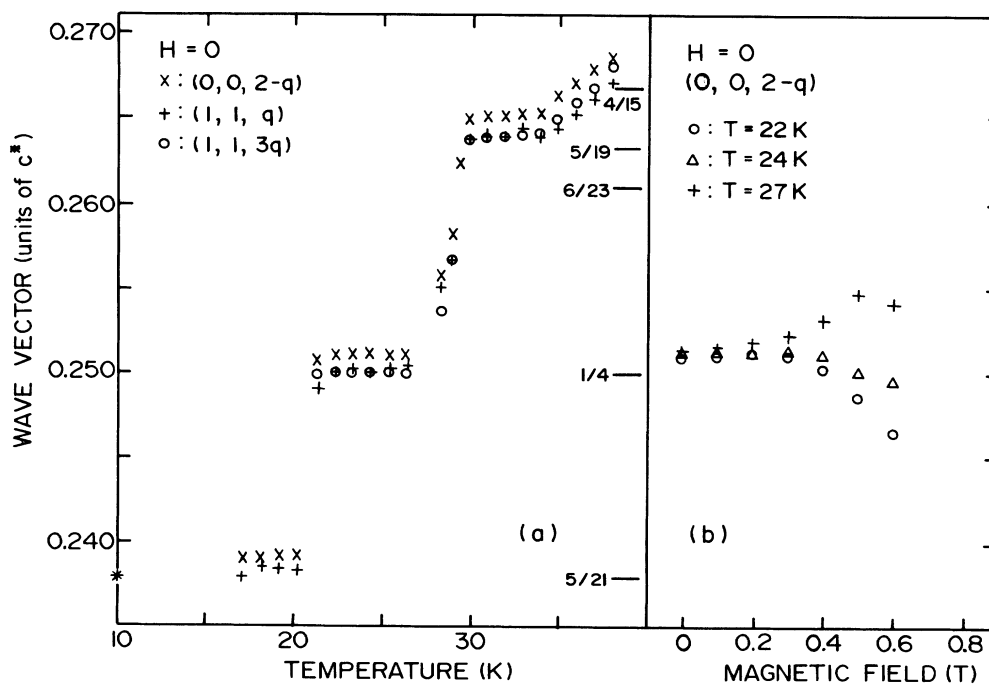


FIG. 2. (a) Lock-ins in zero field along the $[00l]$ and $[11l]$ directions. (b) The wave vector q as a function of field near the $q=(1/4)c^*$ in the intermediate phase.

$q=(1/4)c^*$ phase. The variation of q with field is reversible at 22 K below a field of 0.7 T. Although the figure only shows the $(0,0,2-q)$ reflection, the measured $(1,1,q)$ and $(1,1,3q)$ reflections in fields of 0.5 and 1.0 T also indicate that lock-ins no longer exist for the z component of the moment.

It is interesting to note that $q=4/15$ at about 38 K is an inflection point which is not affected by the fields until 1 T. The inflection behavior in zero field near $q=4/15$ was also observed by Habenschuss *et al.*²

Another feature is that the field stabilizes the lock-in at $q=(2/7)c^*$ at higher temperatures. Figure 3(a) shows two examples where the wave vector is obtained from the $(0,0,2-q)$ reflection. The onset temperature and field of the lock-in in the intermediate phase can be described by $T_L=54.0-5.3H_L$ ($0 < H_L < 1.5$ T) and $T_L=21.0+16.7H_L$ ($1.5 < H_L < 2.2$ T). The measured $(1,1,q)$ reflections also suggest that $q=2/7$ persists in the CAM phase at fields of 1.0 T and above. Not enough data were taken in this phase to determine the full extent of lock-in at $2/7$.

The cone phase is stabilized by the field. The temperature range of the lock-in with $q=(5/21)c^*$ is almost field independent. Above 21 K the magnitude of q is usually reduced as the field is increased at fixed temperature. For fields above 1.8 T and temperatures between 34 and 39 K, we observed a lock-in cone structure with $q=(1/4)c^*$. The cone angle in this phase is about 21° .

Figure 4 shows plots for the lattice constant c obtained from the position of the $(0,0,2)$ nuclear reflection. The change of value c from about 5.60 Å to about 5.58 Å corresponds to the transition from the cone phase to the

spin-slip phase. It is clear that the major determinant of the value of c is the nature of the magnetic phase. Within a phase the field and lock-ins give smaller effects. Small steps at 5.600, 5.580, 5.578, 5.596, and 5.573 are seen, corresponding to the lock-ins of $q=(5/21)c^*$, $(1/4)c^*$, and $(5/19)c^*$ in zero field and $(1/4)c^*$ and $(2/7)c^*$ in a field.

B. Magnetic phase diagram

A series of measurements were made on certain magnetic reflections over a wide range of temperature and field in order to establish the magnetic field-temperature phase diagram. Figure 5 summarizes the results. The dots and the crosses are from experimental data. The solid and dashed lines are guides to the eyes.

The dots in the figure are the phase boundaries as determined from changes in the location or the intensity of the Bragg peaks. The disappearance of the $(1,1,q)$ and the $(0,0,2-q)$ reflections were used to determine the boundary of the CAM phase. Examples of this determination are shown in Fig. 3(b). The phase boundary from the intermediate to the cone phase may be determined in several ways. There is a sudden increase of the intensity of the $(1,1,q)$ reflection [one example at a field of 1.7 T is shown in Fig. 3(b)] and of the $(1,1,2-5q)$ reflection, and a sudden decrease of the intensity of $(1,1,0)$ which describes the ferromagnetic components. The changes are accompanied by a decrease of about 0.4% in the lattice parameter c as was noted by Habenschuss *et al.*² The phase transition takes place from 21 K in zero field to 59 K in a field of 2.5 T and its location is

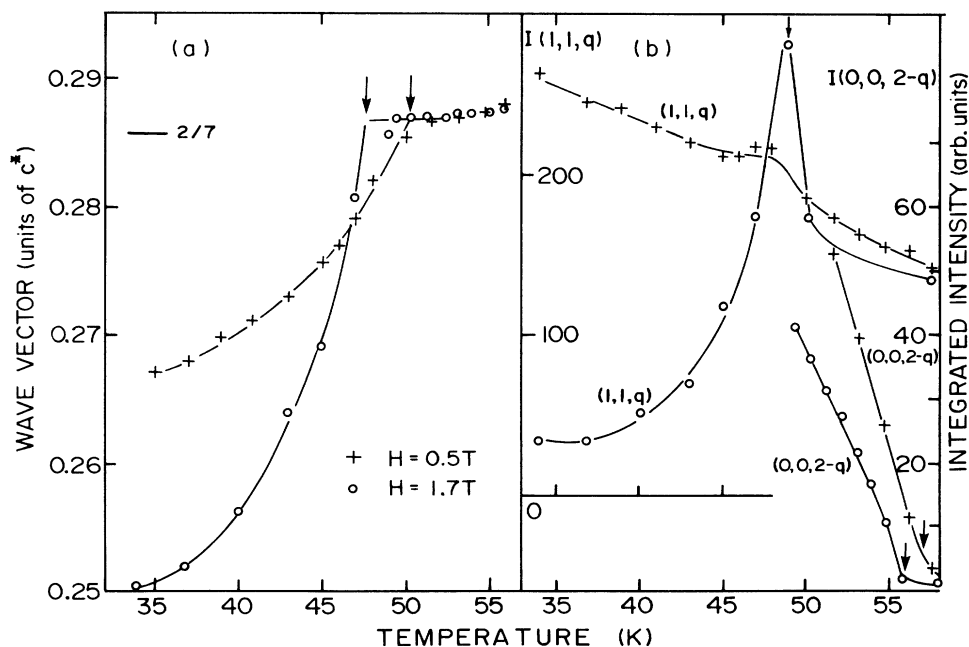


FIG. 3. (a) The lock-in at $2/7$ from the $(0,0,2-q)$ reflection in fields of 0.5 and 1.7 T. (b) Phase transition between the intermediate and the CAM phase reflected by the $(0,0,2-q)$ peak and between the cone and the intermediate phase reflected by the $(1,1,q)$ peak in fields of 0.5 and 1.7 T. The arrow marks the phase transition temperature.

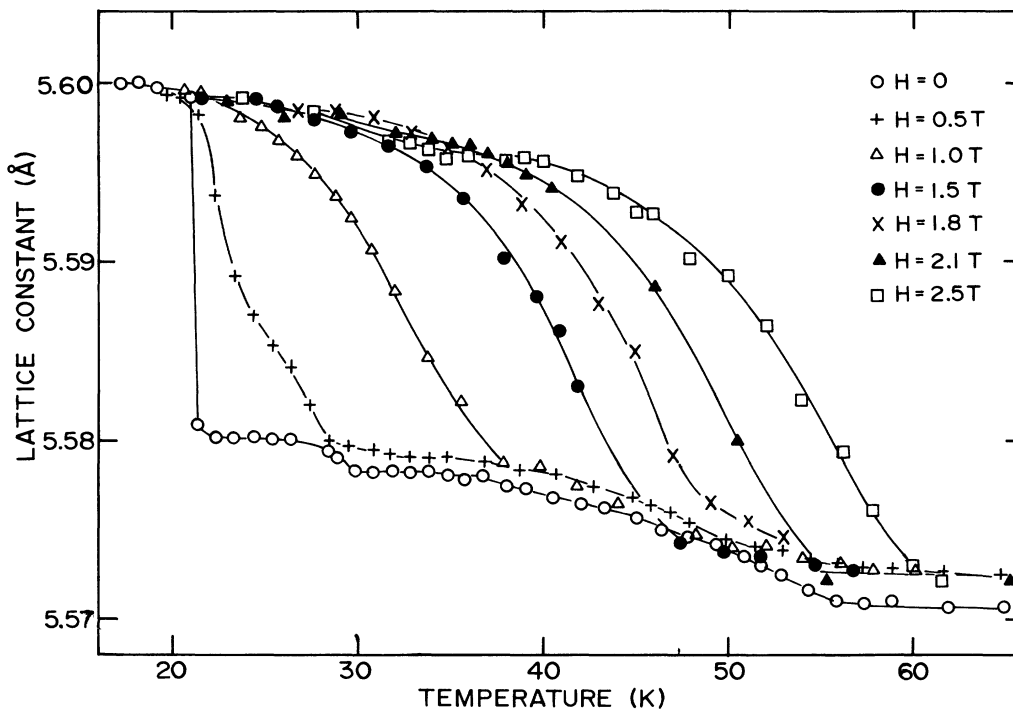


FIG. 4. The lattice parameter c as a function of temperature at different fields along the c axis. The large change in c from about 5.60 to 5.58 Å corresponds to the phase transition from the cone phase to the intermediate phase. Small steps correspond to the lock-ins in the magnetic structure.

consistent with the magnetization measurements.¹⁴ The solid lines in the phase diagram (Fig. 5) are borders between the distinct types of phase. The line marking the high-field limit of the CAM phase is taken from the magnetization data.¹⁴

The crosses in Fig. 5 are experimental points which

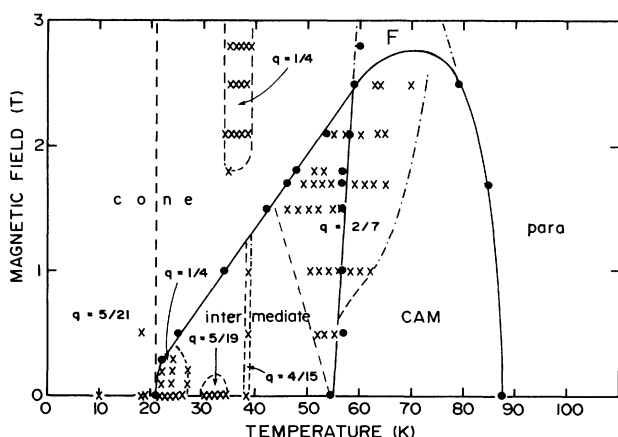


FIG. 5. Magnetic phase diagram with applied field along the c axis. The dots are measurements of the phase transition temperature. The crosses are experimental points corresponding to lock-ins. The lines are guides to the eyes. The solid line is the boundary between two distinct phases. The dashed line is the boundary between commensurate and incommensurate phases. The dashed-dot line corresponds to boundaries whose location has not been accurately determined.

correspond to lock-ins at rational-fractional values of q . We have found six islands, each corresponding to a lock-in, in the sea of incommensurate structures. The dashed lines are boundaries between the commensurate and incommensurate phases. The transition temperature for these lock-ins is determined from data such as that shown in Fig. 3(a). Some of the lock-in regions extend to the boundary between cone and intermediate phases. The phase transition at this boundary can be of three types: incommensurate to commensurate ($H < 0.5$ T; $H > 1.5$ T), commensurate to commensurate ($H = 0$ T), and incommensurate to incommensurate (0.5 T $< H < 1.5$ T except close to 1.3 T).

When the xy components of the moments become disordered, the commensurate structure with the same wave vector, $q = 2/7$, persists through the phase boundary at fields of 1.0 T and above. The experimental data at 2.5 T indicates that q moves away from $2/7$ between 70 and 75 K. This suggests that there may exist a boundary for the $q = 2/7$ island in the CAM phase which is shown by the dashed-dot line in Fig. 5.

Although no data were taken at low temperatures in a magnetic field, extrapolating the data from just above 21 K in Fig. 1 leads to the conclusion that there is a boundary for the $q = (5/21)c^*$ commensurate structure in the cone phase which is temperature independent.

Our measurements show that the line on the phase diagram marking the transition from order to disorder of moments in the ab plane persists above 2.5 T. This suggests that the region labeled F in Fig. 5 corresponds to a ferromagnetic phase.

C. Magnetic structures

1. CAM phase

A survey with \mathbf{Q} in the range of $(0,0,0.1)$ to $(0,0,4)$ and $(1,1,-0.44)$ to $(1,1,2.44)$ was conducted for fields of 0, 1.7, and 2.1 T at a temperature of 65 K and for a field of 2.5 T at 70 and 78 K. The average value of q is 0.292 ± 0.002 , 0.287 ± 0.003 , 0.288 ± 0.002 , 0.285 ± 0.003 , and 0.279 ± 0.003 , respectively. Only the first and last of these five values are significantly different from $2/7$ (0.286). The ratio of intensity of the first-order magnetic satellites to the nuclear peaks along $[00l]$ for all the data is not greater than 0.5%, which is consistent with no magnetic ordering in the ab plane in this phase.

Higher-order harmonics were observed along $[11l]$. The sole exception is at 2.5 T and 78 K where the structure is sinusoidal. As the temperature increases the intensity of the harmonics along the $[11l]$ direction falls faster than that of the fundamental. This indicates an increasing rounding off of the squared-up structure of the moments along c as the temperature increases. Near the Néel temperature the structure is close to being sinusoidal.

The c -axis spin-slip model³ was applied to the $\mathbf{q}=(2/7)\mathbf{c}^*$ phase. We note that spin-slips form a 4,3 and not a 4,3,3,4 repeat unit since the latter requires that the harmonics at $l=m/7$ with m odd are of the same order of intensity as the harmonic $l=6/7$, which was not observed. However, the measured first-order harmonics are much stronger than predicted for a squared-up structure, so that the squaring up is incomplete. The structure of the phase with $\mathbf{q}=(2/7)\mathbf{c}^*$ can be regarded as a superposition of the squared-up structure and the sinusoidal structure. Table I lists the observed and calculated magnetic structure factors for the $\mathbf{q}=(2/7)\mathbf{c}^*$ phase at 1.7 T and 65 K. The moment associated with the sinusoidal wave is $\mu_0=4.6\mu_B$ and the amplitude of the squared-up structure is $\mu_s=1.5\mu_B$. The 4,3 structure implies a small net ferromagnetic moment, which would be seen in magnetization or polarized neutron experiments. Such a moment is not detectable in our data because its scattering is masked by the nuclear Bragg peaks. The observed peak at $l=5/7$ cannot be described within this model, though the differing intensity of the $(1,1,5/7)$ and the $(1,1,2-5/7)$ reflections is difficult to explain in any model of the type we have examined. However, if a symmetry

breaking occurs that distinguishes between the two sublattices, $[\mathbf{R}=(0,0,0)$ and $\mathbf{R}=(\frac{1}{3}, \frac{2}{3}, \frac{1}{2})]$, the $(1,1,1\pm q)$ reflections [$l=5/7$ in the $\mathbf{q}=(2/7)\mathbf{c}^*$ phase] can be understood if the two sublattices have phase angles differing by about 2.3° .

We should note that all our Bragg peaks, nuclear and magnetic in all phases, have widths that are limited either by the mosaic spread of the sample (transverse scans) or by the instrumental resolution (longitudinal scans). In particular the magnetic peaks corresponding to harmonics have the same width as the fundamental. A similar result has been found in holmium.⁹

2. Cone phase

Application of a magnetic field along the c axis serves to close up the cone angle. The average half angle of the cone in our sample, as determined from the intensity of $(0,0,2-q)$ reflection and from the magnetization data,¹⁵ decreases gradually from 29° at zero field and 10 K to 19° at 2.5 T and 52 K.

In addition to the first-order magnetic satellites, we observed harmonics in this phase which are not described in the earlier literature. Figure 6 shows the diffraction pattern along the $[00l]$ direction on a logarithmic scale at zero field and 10 K where q is locked in at $5/21$. The harmonic peaks can be indexed as $(0,0,2n\pm 1/21)$ and $(0,0,2n\pm 11/21)$ and would correspond to 17th and 19th harmonics, respectively, of the fundamental $(0,0,2n\pm 5/21)$. As suggested by Gibbs *et al.*³ and Bohr *et al.*¹⁶ the $\mathbf{q}=(5/21)\mathbf{c}^*$ structure can be described by a basal-plane spin-slip model. There are three slips every seven atomic layers, and the pattern repeats six times. If “.” is a single spin and “1” is a pair of spins, they have proposed that $(\cdot\cdot 1\cdot)^6$ is the spin configuration in the basal plane. The single spin lies on the easy axis and a pair of spins deviates from the easy axis by an angle $\pm\alpha$. The insert to Fig. 6 shows the first eight layers of this basal-plane-spin-slip model. Another alternative arrangement is $(\cdot 11\cdot\cdot)^6$ where two pairs are close. However, the latter contributes too much intensity to the harmonics and may be ruled out by our results. Table II shows the calculated structure for the $(\cdot\cdot 1\cdot)^6$ configuration with $\alpha=2\pi/17=21.2^\circ$ and with the z component of the moments ferromagnetically aligned. The model generates harmonic peaks at $(h,k,2n\pm m/21)$ with $m=1,7,11,13,19$. α has been chosen so that the har-

TABLE I. Square of the magnetic structure factor relative to the nuclear structure factor in erbium at 65 K and 1.7 T in the CAM phase locked in at $q=2/7$. The calculated values correspond to a superposition of the squared-up $\uparrow\uparrow\uparrow\uparrow\downarrow\downarrow$ (4,3) structure and a sinusoidal structure with the same period.

l	$ F_z^m(\mathbf{Q})/F^n(\mathbf{Q}) ^2$								
	0/7	1/7	2/7	3/7	4/7	5/7	6/7	7/7	
Obs.									
1,1,2+l	0	0.00	15						
1,1,2-l	0	0.00	16	0.00	0.15	0.24	0.14	0.00	
1,1,0+l	0	0.00	15	0.00	0.17	0.01	0.15	0.00	
Average	0±2	0.00±0.01	15±2	0.00±0.01	0.16±0.02	0.13±0.10	0.15±0.02	0.00±0.02	
Calc.	0.08	0	15.3	0	0.09	0	0.19	0	

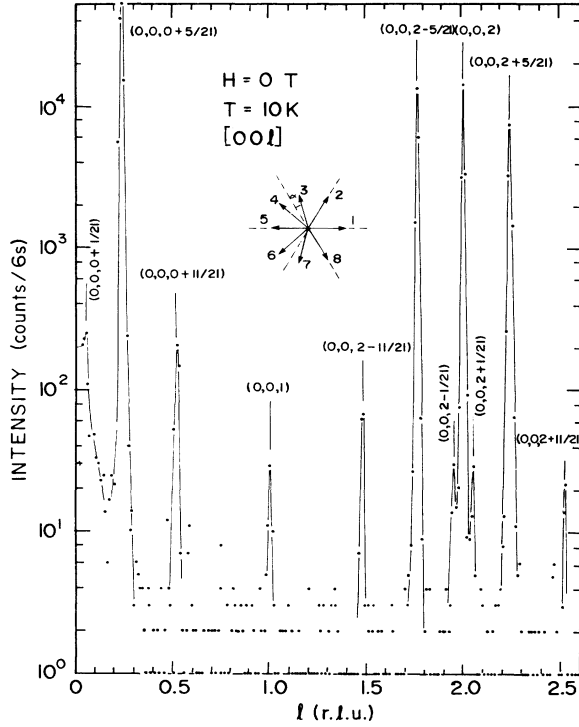


FIG. 6. Diffraction pattern from the $q=(5/21)c^*$ phase at 0 T and 10 K along the $[00l]$ direction. The insert shows the first eight layers of the basal-plane spin-slip model for this structure.

monics with $m=1$ and 11 have the strongest intensity. There is reasonable agreement with experiment.

Unexpectedly the forbidden nuclear peak (1,1,1) was observed in all structures of the cone phase, an example can be seen in Table II. This was also noted by Rhyne and Pickart.⁴ If the peak is magnetic in origin, its intensity corresponds to a moment of about $1.6\mu_B$ along the c axis and its existence implies different moments in the c direction for the ferromagnetic planes at $z=nc$ and at $z=(2n+1)c/2$ with n an integer. This seems implausible: the alternative is that the peak is nonmagnetic in origin. In this case its existence implies a lowering of the

hcp symmetry, presumably induced by magnetostrictive effects.

The Bragg peak at the $(1,1,1\pm 5/21)$ position, is also not explained by the spin-slip model. It could be a satellite to a nuclear (1,1,1) peak. Alternately it is possible that the z component of the moments is modulated, though our data are rather insensitive to this effect.

Weak harmonics of type $(0,0,2n\pm 0.532)$ were observed in the incommensurate cone phase with $q=(0.242\pm 0.001)c^*$ at 1.5 T and 23 K. These harmonics correspond to $(11/5)q$. In the commensurate cone phase with $q=(0.250\pm 0.002)c^*$ at 2.5 T and 36 K weak $(0,0,2n\pm 1/2)$ peaks were observed. Although the ratio of their intensity to the first-order magnetic satellites is 0.5–1.5%, they were only seen in the cone phase and in the intermediate phase with $q=(1/4)c^*$ in zero field.

The basal-plane spin-slip model, shown as the inset of Fig. 6, with $\alpha=18^\circ$, can give a qualitative explanation of the data for the commensurate cone phase with $q=(1/4)c^*$ at 2.5 T and 36 K.

3. Intermediate phase

Surveys were taken along $[00l]$ and $[11l]$ for $q=(2/7)c^*$ at 2.1 T and 55 K; for $q=(1/4)c^*$, $q=(5/19)c^*$, and $q=(0.277\pm 0.002)c^*$ at 0 T and 23, 33, and 46 K, respectively.

Figures 7(a) and 7(b) show the diffraction pattern of the phase with $q=(1/4)c^*$ in zero field. As was the case with the low-temperature cone phase, magnetic satellites were observed corresponding to harmonics. The appearance of the harmonic with $q=(2/4)c^*$ suggests that the basal-plane spin-slip model may also be applied to the xy components of the moments in this phase. The scattering from the z component of the moments is consistent with a structure that has four layers of “up” spins followed by four layers of “down” spins. Table III gives a comparison of the experiment and the theory. The fitted value of the moment is $\mu_{xy}=4.3\mu_B$ in the basal plane and $\mu_z=7.3\mu_B$ along the c axis. The pattern of the spin-slips in the basal plane is shown as the insert of Fig. 7(a) with $\alpha=3^\circ$. This model is in agreement with the experimental data.

TABLE II. Square of the magnetic structure factor relative to the nuclear structure factor in erbium at 10 K and zero field. This corresponds to the cone phase with $q=(5/21)c^*$. The calculated values are for a ferromagnetic moment of $7.0\mu_B$ along the c axis and a moment of $4.5\mu_B$ in the basal plane rotating according to the spin-slip model.

l	$ F_{xy}^m(\mathbf{Q})/F^n(\mathbf{Q}) ^2$					$ F_z^m(\mathbf{Q})/F^n(\mathbf{Q}) ^2$	
	1/21	5/21	11/21	13/21	19/21	0	16/21
Obs.							
0,0,2+l	0.05	16	0.05	0.00	0.00		
0,0,2-l	0.04	19	0.07	0.00	0.00		
0,0,0,+l	0.09	12	0.09	0.00	0.00		
1,1,2-l		12	0.08	0.00	0.00	70	0.8
1,1,0+l		11	0.09	0.00	0.00	81	0.2
1,1,1							3.4
Average	0.06 ± 0.02	14 ± 3	0.08 ± 0.02	0.00 ± 0.01	0.00 ± 0.1	76 ± 6	
Calc.	0.06	15.6	0.05	0.02	0.01	76	0

As the temperature increases, the intensity of the harmonics along the $[11\bar{1}]$ direction falls faster than that of the fundamental. The temperature dependence of these harmonics has been studied in detail by Habenschuss

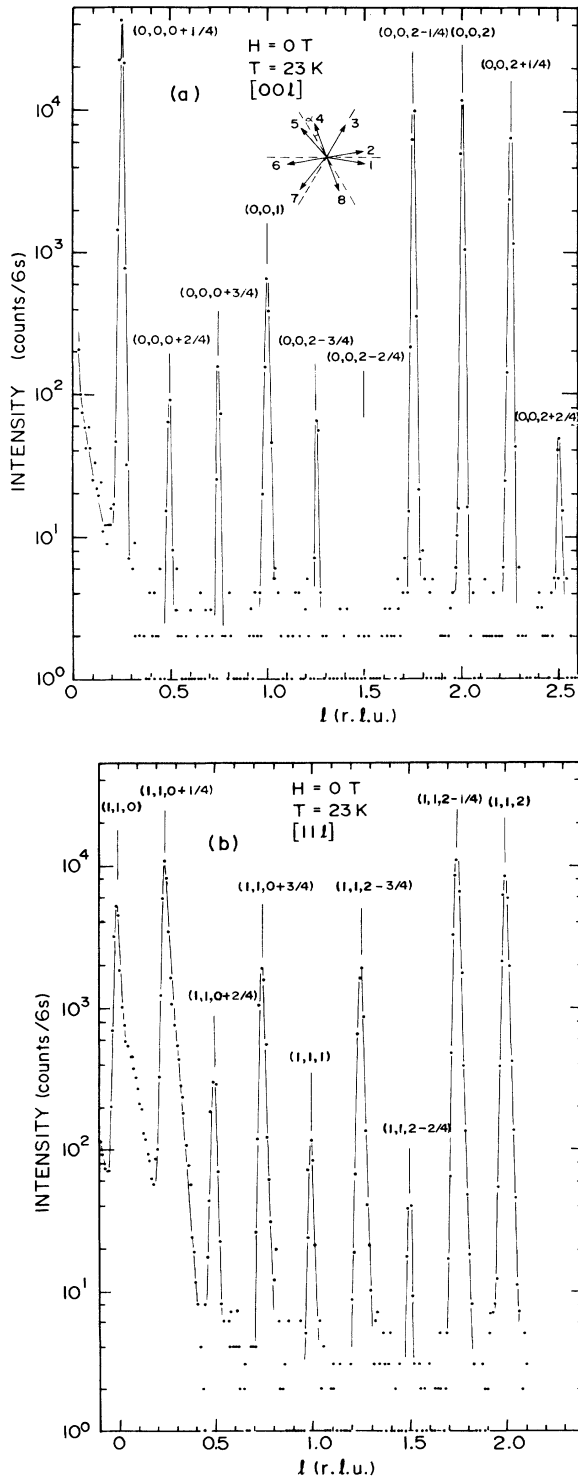


FIG. 7. Diffraction pattern of the intermediate phase locked in at $q=(1/4)c^*$ with zero field and a temperature of 23 K, along (a) the $[00\bar{1}]$ and (b) the $[11\bar{1}]$ direction. The insert shows the basal-plane spin slips.

*et al.*² Our data both in the $q=(5/19)c^*$ and the $q=(0.277\pm 0.002)c^*$ phases show that the intensities of the harmonics are weaker than those predicted by the c -axis spin-slip model. This indicates an increasing rounding off of the squared-up structure of the z component of moments as the temperature increases. Along the $[00\bar{1}]$ direction, no harmonics were observed for the $q=(2/7)c^*$ phase. Third and fifth harmonics were seen for the $q=(5/19)c^*$ and the $q=(0.277\pm 0.002)c^*$ phase. However, it is difficult to find any spin-slip pattern in the basal plane to explain all the observed harmonics in the latter two phases. This implies a breaking-down of the basal-plane spin-slip model as the temperature rises.

We note that the $(0,0,1)$ peak has significant intensity in all structures of the intermediate phase. Its intensity is 1.5–5 % of that of the $(0,0,2)$ nuclear peak, a value that is much larger than the observed 0.2% in the cone phase which arises from $\lambda/4$ contamination of the beam. If we postulate that the intensity of the $(1,1,1)$ peak arises solely from the scattering of the moment in the basal plane, the intensity of the $(0,0,1)$ peak is still considerably larger than would be produced by this basal plane moment. An example is given in Table III. Therefore the major component of the scattering from $(0,0,1)$ is likely to be nuclear rather than magnetic scattering. There must be a lowering of hcp symmetry caused presumably by the magnetostriction.

The question of the nuclear or magnetic origin of the $(0,0,1)$ and $(1,1,1)$ peaks can be resolved by x-ray or polarized-neutron measurements.

V. DISCUSSION

The complicated magnetic structure and phase diagram of erbium results from the competition between the exchange, crystal-field anisotropy, magnetoelastic, and applied field energies.^{17–20} Our experiments give new results concerning the effect of a magnetic field along c on the magnetic structure.

In the cone phase, the existence of weak harmonics along the $[00\bar{1}]$ direction indicates that the xy components of the moments, ferromagnetically aligned within the basal planes, do not rotate uniformly from layer to layer along the c axis. The agreement between the experiment and the basal-plane spin-slip model for the $q=(5/21)c^*$ structure in zero field suggests that the moments are influenced by a hexagonal anisotropy in the ab plane. Although this anisotropy energy is less than the energy of the axial anisotropy, it is nonetheless important in determining the lock-ins. An alternative treatment of the hexagonal anisotropy without spin slip²¹ predicts that the fifth and seventh harmonics will be observed and does not fit our data.

A model with completely squared-off c -axis moments and basal-plane spin-slips gives a reasonable explanation of the data for the $q=(1/4)c^*$ structure in the intermediate phase. As the temperature is increased, the hexagonal anisotropy becomes less important. The driving forces for the lock-in to commensurate phases are the axial anisotropy of crystal field and the magnetostriction. The lock-ins are primarily determined by the z com-

TABLE III. Square of the magnetic structure factor relative to the nuclear structure factor in erbium at 23 K and zero field, and $G^2 \equiv (1 + \hat{Q}_z^2) |F_{xy}^m(\mathbf{Q})/F^n(\mathbf{Q})|^2 + (1 - \hat{Q}_z^2) |F_z^m(\mathbf{Q})/F^n(\mathbf{Q})|^2$. The data are for the spin-slip phase with $\mathbf{q} = (1/4)\mathbf{c}^*$. The calculated values correspond to a squared-up $\uparrow\uparrow\uparrow\downarrow\downarrow\downarrow$ (4,4) structure along the c axis and the basal-plane spin-slip model.

l	$ F_{xy}^m(\mathbf{Q})/F^n(\mathbf{Q}) ^2$				
	0	1/4	2/4	3/4	4/4
Obs.					
0,0,4- l		13	0.00	0.15	0.16
0,0,2+ l	0	14	0.12	0.08	
0,0,2- l		16	0.00	0.06	(0.52)
0,0,0+ l		11	0.2	0.08	
Average	0±1	13±2	0.03±0.04	0.09±0.03	0.16±0.03
Calc.	0.14	14	0.10	0.06	0.14
			G^2		
l	0	1/4	2/4	3/4	4/4
Obs.1,1, l	0±1	42±4	0.12±0.02	6.9±0.4	0.12±0.03
Calc.	0.14	49	0.11	5.8	0.15
Obs.1,1,2- l	0±1	42±4	0.15±0.02	6.7±0.4	0.12±0.03
Calc.	0.18	44	0.12	5.3	0.15

ponent of the moments. The structures with $\mathbf{q} = (2/7)\mathbf{c}^*$ and $\mathbf{q} = (5/19)\mathbf{c}^*$ show an incomplete squared-up z component of the moments. The model takes care of a difficulty that early workers^{1,2} had, in that the structures which it predicts have no atom with a moment greater than allowed by theory.

The effect of field along the c axis on the lock-ins is interesting and supports the contention above that the lock-ins are primarily determined by the z component of the moment. The extent of the $\mathbf{q} = (5/21)\mathbf{c}^*$ cone phase at low temperatures is unaffected by the field. A new lock-in appears in the cone phase at $\mathbf{q} = (1/4)\mathbf{c}^*$ for fields above 1.8 T. In the intermediate phase, the $\mathbf{q} = (5/19)\mathbf{c}^*$ lock-in is destroyed rapidly, the $\mathbf{q} = (4/15)\mathbf{c}^*$ lock-in is sustained, and the $\mathbf{q} = (2/7)\mathbf{c}^*$ lock-in is extended considerably. The latter two structures possess small net magnetic moments parallel to the c axis, so it seems that lock-ins with ferrimagnetism along the c axis are stabilized by the field. There is no evidence that the field modifies the configuration of the spin-slip structures.

The field and temperature dependence of magnetic structure is described in the magnetic phase diagram. At least three distinct types of ordered phase, the cone phase, the intermediate phase, and the CAM phase exist for fields below 2.5 T. The boundary between the intermediate and the CAM phase is almost field independent. This indicates that the field along the c axis has little influence on the xy components of the moments. The wave vector q , in general, increases with increasing temperature and decreases with increasing field.

A mean-field theory of the magnetic structure of erbium was proposed by Elliott.²² The temperature dependence of the wave vector was calculated by Elliott and Wedgewood²³ based on a model using an exchange interaction between localized moments and the conduction

electrons. The magnetization was calculated by Jensen²⁴ considering crystal-field anisotropy and the interplanar exchange parameters as deduced from the spin wave dispersion.²⁵

A soliton theory based on the axial next-nearest-neighbor Ising (ANNNI) model was suggested by Bak and Boehm²⁶ to explain the lock-in for the z components of the moment by a "devil's-staircase" mechanism. This model is clearly incomplete for erbium because it does not take into account the xy components of the moments. It predicts the low-temperature structure of the z components of the moment to be the 1/4 structure ($\uparrow\uparrow\uparrow\downarrow\downarrow\downarrow$). The strength of the model is that it does give a basis for explaining the succession of lock-ins as the temperature is varied at zero field.

In conclusion, we believe that there is ample evidence that the ideas of Jensen,²⁴ (regarding the basic interactions), of Bak and Boehm²⁶ (regarding the devil's staircase for the z component of the moment), and of Bohr *et al.*¹⁶ (regarding spin slips in the xy plane) are appropriate for erbium. To explain the experimental data it is probably necessary to find a model that incorporates all these features.

ACKNOWLEDGMENTS

We are grateful to W. J. L. Buyers, R. A. Cowley, and A. R. Mackintosh for useful discussions. We are indebted to C. V. Stager for independently verifying our temperature scales. We thank P. A. Moss, H. F. Nieman, D. C. Tennant, and M. M. Potter for technical assistance with the experiments at Chalk River. H.L. and M.F.C. acknowledge the financial support of the Natural Sciences and Engineering Research Council Of Canada.

- ¹J. W. Cable, E. O. Wollan, W. C. Koehler, and M. K. Wilkinson, *Phys. Rev.* **140**, A1896 (1965).
- ²M. Habenschuss, C. Stassis, S. K. Sinha, H. W. Deckman, and F. H. Spedding, *Phys. Rev. B* **10**, 1020 (1974).
- ³D. Gibbs, J. Bohr, J. D. Axe, D. E. Moncton, and K. L. D'Amico, *Phys. Rev. B* **34**, 8182 (1986).
- ⁴J. J. Rhyne and S. J. Pickart, in *Magnetism and Magnetic Materials 1971 (Chicago)*, Proceedings of the 17th Annual Conference on Magnetism and Magnetic Materials, AIP Conf. Proc. No. 5, edited by D. C. Graham and J. J. Rhyne (AIP, New York, 1972), p. 1436.
- ⁵M. Atoji, *Solid State Commun.* **14**, 1047 (1974).
- ⁶R. S. Eccelstone and S. B. Palmer, *J. Magn. Magn. Mater.* **104-107**, 1529 (1992).
- ⁷H. Lin, M. F. Collins, T. M. Holden, and W. Wei, *J. Magn. Magn. Mater.* **104-107**, 1511 (1992).
- ⁸D. C. Tennant, N. Kerley, and N. Killoran, *Rev. Sci. Instrum.* **60**, 136 (1989).
- ⁹R. A. Cowley and S. Bates, *J. Phys. C* **21**, 4113 (1988).
- ¹⁰C. Stassis, G. R. Kline, A. J. Freeman, and J. P. Desclaux, *Phys. Rev. B* **13**, 3916 (1976).
- ¹¹V. F. Sears, in *Methods of Experimental Physics 23(A), Neutron Scattering*, edited by K. Sköld and D. L. Price (Academic, Orlando, Florida, 1986), p. 521.
- ¹²N. Ali and F. Willis, *Phys. Rev. B* **42**, 6820 (1990).
- ¹³H. U. Astrom, D. X. Chen, G. Benediktsson, and K. V. Rao, *J. Phys. Condens. Matter* **2**, 3349 (1990).
- ¹⁴S. Gama and M. E. Foglio, *Phys. Rev. B* **37**, 2123 (1988).
- ¹⁵J. L. Feron, G. Hug, and R. Pauthenet, *Z. Angew. Phys.* **30**, 61 (1970).
- ¹⁶J. Bohr, D. Gibbs, D. E. Moncton, and K. L. D'Amico, *Physica* **140A**, 349 (1986).
- ¹⁷*Handbook of the Physics and Chemistry of Rare Earth*, edited by K. A. Gschneidner, Jr. and L. R. Eyring (North-Holland, Amsterdam, 1978), Vol. 1.
- ¹⁸*Magnetic Properties of Rare Earth Metals*, edited by R. J. Elliott (Plenum, New York, 1972).
- ¹⁹B. Coqblin, *The Electronic Structure of Rare-Earth Metals and Alloys: the Magnetic Heavy Rare-Earths* (Academic, London, 1977).
- ²⁰J. Jensen, and A. R. Mackintosh, *Rare Earth Magnetism: Structure and Excitations* (Oxford University Press, Oxford, 1991).
- ²¹H. Miwa and K. Yosida, *Progr. Theor. Phys.* **26**, 693 (1961).
- ²²R. J. Elliott, *Phys. Rev.* **124**, 346 (1961).
- ²³R. J. Elliott and F. A. Wedgwood, *Proc. Phys. Soc.* **84**, 63 (1964).
- ²⁴J. Jensen, *J. Phys. F* **6**, 1145 (1976).
- ²⁵R. M. Nicklow, N. Wakabayashi, M. K. Wilkinson, and R. E. Reed, *Phys. Rev. Lett.* **27**, 334 (1971).
- ²⁶P. Bak and J. von Boehm, *Phys. Rev. B* **21**, 5297 (1980).